

HIGHER-ORDER SPECTRA IN NANOPARTICLE GAS SENSORS

J. M. SMULKO^{*,†,‡}, J. EDERTH^{*,†}, L. B. KISH[‡], P. HESZLER^{*,§} and C. G. GRANQVIST^{*}

^{*}*Department of Engineering Sciences, The Ångström Laboratory, Uppsala University,
P.O. Box 534, SE-751 21 Uppsala, Sweden*

[†]*Gdansk University of Technology, WETiI, ul. G. Narutowicza 11/12, 80-952 Gdansk, Poland*

[‡]*Department of Electrical Engineering, Texas A&M University, College Station,
TX 77843-3128, U.S.A.*

[§]*Research Group of Laser Physics of the Hungarian Academy of Sciences,
University of Szeged, P.O. Box 406, H-6701 Szeged, Hungary*

Received 15 September 2004

Revised 15 October 2004

Accepted 19 October 2004

Communicated by Boris M. Grafov

It has previously been shown that resistance fluctuations in resistive sensors provide enhanced sensitivity and selectivity for gas detection. We report measurements and analysis of non-Gaussian components in nanoparticle $\text{Pd}_z(\text{WO}_3)_{1-z}$ film gas sensors, with z being 0.01 or 0.12, in different ambients. These components can be characterized by higher-order spectra. Contour plots are given of bispectra, and plots of integrated bispectra and trispectra. The phase of the integrated higher-order spectra is analyzed as well.

Keywords: Gas sensor; gas detection; resistance fluctuation; signal processing; pattern generation; nanoparticle; tungsten oxide.

1. Introduction

Resistive gas sensors can be considered as sources of signals comprising two different components: dc resistance (classical signal) and its fluctuations (stochastic signal) [1]. It has been shown that the stochastic signal component $x(t)$ is a valuable source of information that can be used to improve gas detection by a single gas sensor [1–5]. It is often assumed that the stochastic process is Gaussian, and therefore its analysis is limited to measuring the power spectral density $S_x(f)$ [1–3], where f denotes frequency. However, a strong presence of non-Gaussian components is expected in sensors with small volume or inhomogeneous current density, and experimental studies have indicated [5,6] that non-Gaussian stochastic components are present even in commercial Taguchi sensors as a consequence of their strongly inhomogeneous structure. Analysis of these non-Gaussian components can significantly improve the sensitivity and selectivity of gas

sensors [5,6]. In the earlier studies [5,6], the only higher order spectrum investigated was the bispectrum.

In the present exploratory study, we expand our investigations of nanoparticle films to encompass the integrated bispectrum and trispectrum [7]. Similarly to the earlier studies [1–6], resistance fluctuations were used as the source of stochastic signal.

2. Higher-order Spectra

A stationary stochastic signal $x(t)$, or its sampled time series $x(n)$, is commonly characterized by its power density spectrum. However, an important deficiency of $S_x(f)$ is that it cannot distinguish between Gaussian and non-Gaussian signal components, but such a separation can be accomplished by higher-order spectra.

The bispectrum of a stationary signal is a function of two frequencies f_1, f_2 . It is defined by

$$S_{3x}(f_1, f_2) = \sum_{k=-\infty}^{\infty} \sum_{l=-\infty}^{\infty} C_{3x}(k, l) e^{-j2\pi f_1 k} e^{-j2\pi f_2 l}, \tag{1}$$

where $C_{3x}(k, l) = E[x(n)x(n+k)x(n+l)]$ is the third-order autocorrelation function of $x(n)$, and the operator $E[.]$ denotes averaging. The definition of the bispectrum, which is the function of two equivalent frequencies, implies a few axis symmetries. Thus the bispectrum is unambiguously determined only by a segment of its frequency plane. The lack of advisable symmetries means non-stationarity of the analyzed fluctuations. The bispectrum function vanishes when the skewness of the amplitude density of the signal is equal to that of Gaussian signals.

The trispectrum $S_{4x}(f)$ is a function of three frequencies. It vanishes when the peakedness of the amplitude density of the signal is equal to that of Gaussian signals. It is defined by the equation

$$S_{4x}(f_1, f_2, f_3) = \sum_{i=-\infty}^{\infty} \sum_{k=-\infty}^{\infty} \sum_{l=-\infty}^{\infty} C_{4x}(i, k, l) e^{-j2\pi f_1 i} e^{-j2\pi f_2 k} e^{-j2\pi f_3 l}, \tag{2}$$

where

$$\begin{aligned} C_{4x}(i, k, l) = & E[x(n)x(n+i)x(n+k)x(n+l)] \\ & - E[x(n)x(n+i)]E[x(n+k)x(n+l)] \\ & - E[x(n)x(n+k)]E[x(n+l)x(n+i)] \\ & - E[x(n)x(n+l)]E[x(n+k)x(n+i)] \end{aligned} \tag{3}$$

is the fourth-order autocorrelation function of $x(n)$.

It is worth mentioning that, for a given number of stochastic data, the power spectrum shows significantly lower variance than the bispectrum or the trispectrum. To reduce this variance, the *integrated higher-order spectra* can be used according to [9]

$$S_{3x,I}(f) = \int_{-1/2}^{1/2} S_{3x}(f, f_2) df_2, \quad (4)$$

$$S_{4x,I}(f) = \int_{-1/2}^{1/2} \int_{-1/2}^{1/2} S_{4x}(f_1, f, f_3) df_1 df_3, \quad (5)$$

where $S_{3x,I}(f)$ and $S_{4x,I}(f)$ are the integrated bispectrum and trispectrum, respectively. It is important to note that the integrated spectra shown above are one-dimensional functions, and thus their potential information content is lower, assuming an infinite number of data.

It is interesting to note that the integrated spectra can be calculated as cross spectra from

$$S_{3x,I}(f) = S_{yx}(f), \quad (6)$$

$$S_{4x,I}(f) = S_{rx}(f), \quad (7)$$

where

$$y(n) = x^2(n) - E[x^2(t)], \quad (8)$$

$$r(n) = x^3(n) - 3x(n)E[x^2(t)]. \quad (9)$$

The cross spectra $S_{yx}(f), S_{rx}(f)$ can be estimated by dividing the sample sequence into blocks and averaging the block-sample estimators over the blocks. This is identical to the Welch method of power spectrum density estimation [11]. Different time windows can be used for the blocks, which lead to small differences in variance of the estimated cross spectra.

3. Nanoparticle Sensor Films

Films of $\text{Pd}_z(\text{WO}_3)_{1-z}$ were deposited onto Al_2O_3 substrates with preprinted Au contacts by gas evaporation [8], using independent evaporation sources for Pd and WO_3 . The back side of the substrate had a patterned Pt heating resistor. Two separate batches of sensor samples were prepared with different Pd contents: batch A with ~1 % of Pd, and batch B with ~12 % of Pd. A post-deposition burn-in process of the gas-sensitive films was executed at 600 °C and atmospheric pressure of synthetic air for 1 h. This process developed structurally stable nanoparticle films for gas measurements at temperatures up to 350 °C. The nanoparticle structure consisted of monoclinic WO_3 grains with sizes of ~35 nm. The pristine Pd nanoparticles oxidized during the burn-in process to PdO, and their grain size grew concomitantly from ~5 to ~35 nm. The quoted data were verified by use of scanning electron microscopy.

4. Measurements and Results

Details of the measurement set-up are described elsewhere [6]. It consists of a gas mixer, a stainless steel sensor chamber, a low-noise voltage preamplifier, an AD Instruments PowerLab Data Acquisition system, and a personal computer. The sensor films were polarized with a constant DC voltage from a battery. The flow of gases was controlled

electronically and kept constant. Measurements were conducted with the following gas mixtures:

- synthetic air,
- ethanol (~70 ppm) in synthetic air,
- hydrogen (6 ppm) in synthetic air.

The velocity of the gas flow was kept below 0.3 l/min to avoid turbulence-related temperature fluctuations in the sensor. The stochastic signal data were recorded at a sampling frequency of 10 kHz. The gas sensor was heated during the measurements and kept at a constant temperature of 350 °C.

The amplitude distribution had a non-Gaussian component which changed when the gas composition was altered, as evident from the data shown in Fig. 1. The observed non-Gaussian components are stronger than in commercial Taguchi sensors [6], a fact which probably can be attributed to nanoscale inhomogeneities of the current density distribution in the presently investigated films.

We analyzed bispectra of the recorded data. Figure 2 shows a cross-level contour plot of the absolute value of the bispectrum function of the stochastic signal (batch B) in synthetic air, ethanol (65 ppm), and hydrogen (6 ppm). The large information content of these patterns is indicated by the strikingly different patterns.

Figure 3 shows the cross spectra $S_{yx}(f)$ and $S_{rx}(f)$, which are identical with the integrated bispectrum and trispectrum, respectively. The phases of $S_{yx}(f)$ and $S_{rx}(f)$ were different only for sensors from batch A, as apparent from Fig. 4.

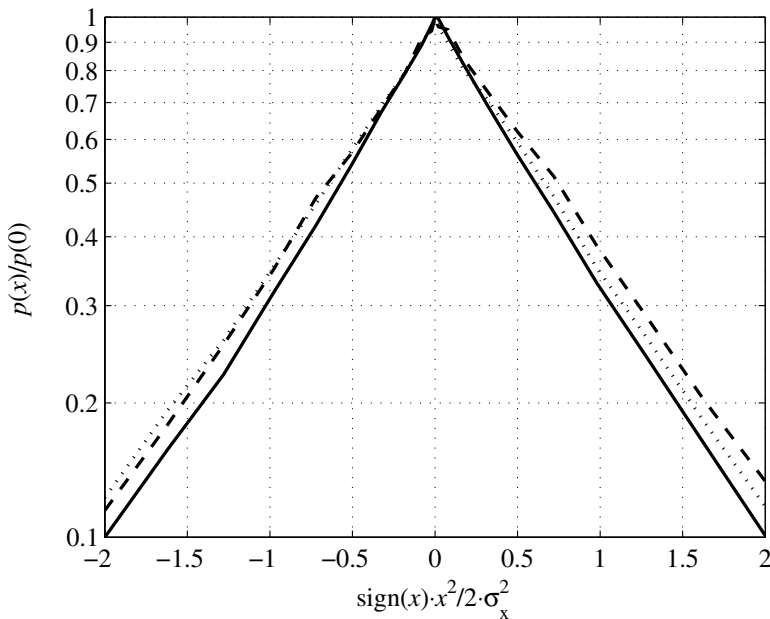


Fig. 1. Normalized amplitude distribution $p(x)/p(0)$ of voltage fluctuations in a sensor from batch B at different ambient gas mixtures: synthetic air (solid line), ethanol 65 ppm (dotted line), hydrogen 6 ppm (dashed line).

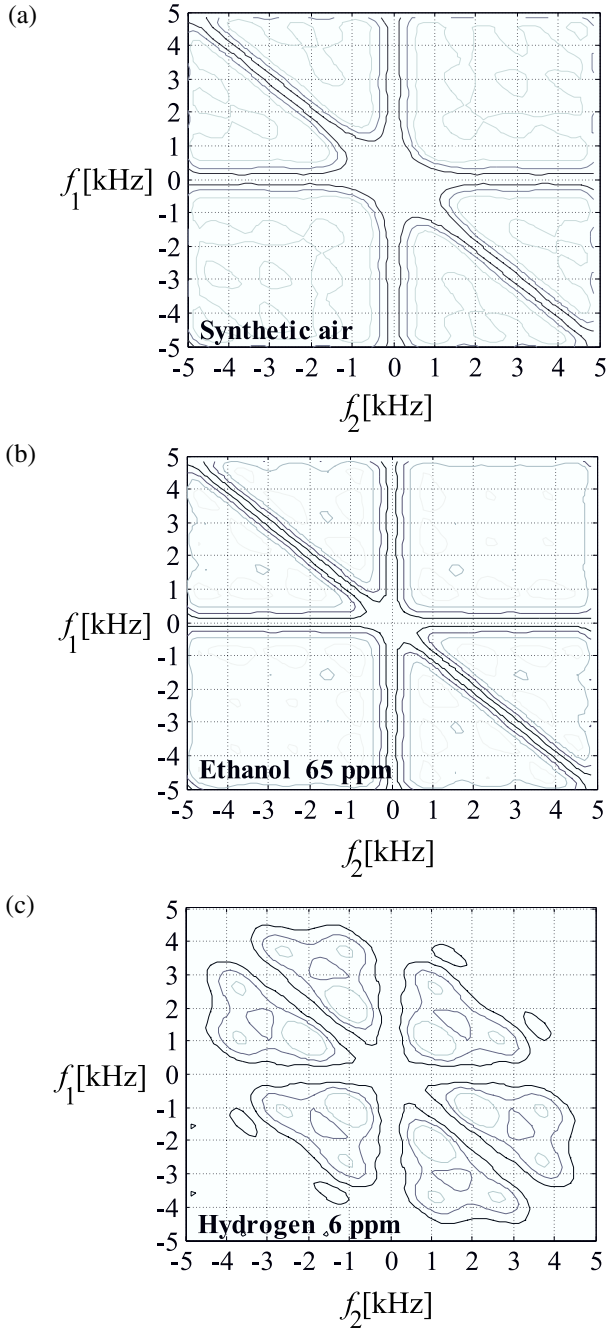


Fig. 2. Cross-level contour plots of absolute values of the bispectrum function of voltage fluctuations in a nanoparticle sensor (batch B) with various ambient gas mixtures: (a) synthetic air, (b) ethanol 65 ppm, and (c) hydrogen 6 ppm.

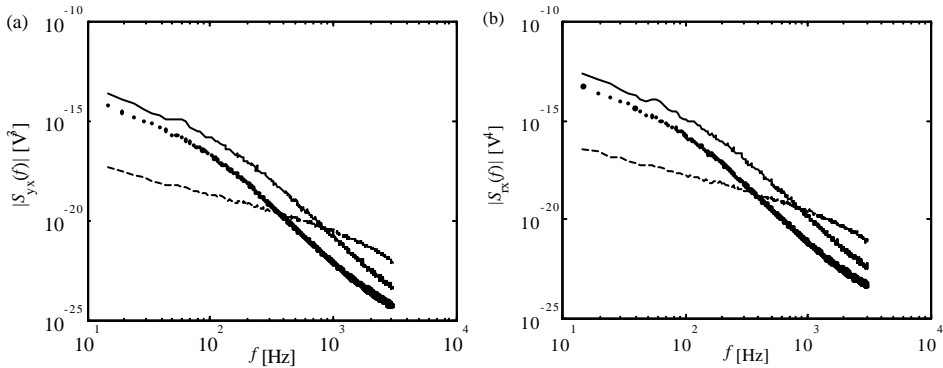


Fig. 3. Absolute value of (a) integrated bispectrum and (b) integrated trispectrum of voltage fluctuations in a nanoparticle sensor (batch B) in various ambient gas mixtures: synthetic air (solid line), ethanol 70 ppm (dotted line), and hydrogen 6 ppm (dashed line).

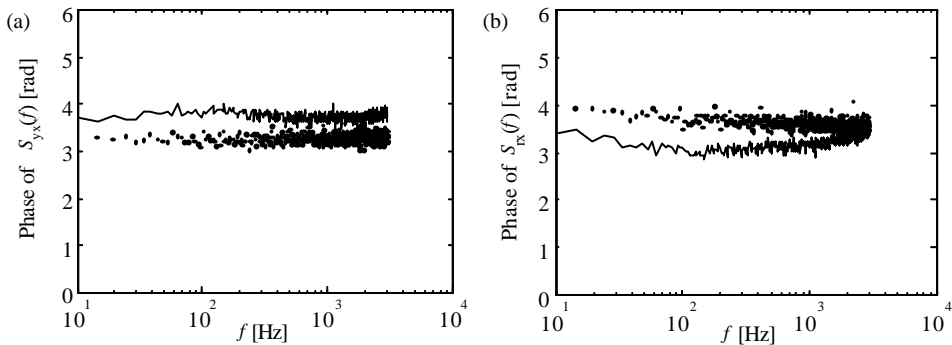


Fig. 4. Phase of (a) integrated bispectrum and (b) integrated trispectrum of voltage fluctuations in a nanoparticle sensor (batch A) with various ambient gas mixtures: synthetic air (solid line), and ethanol 70 ppm (dotted line).

5. Conclusion

The present paper tested the application of higher-order spectral tools for gas recognition in nanoparticle sensors. The experimental study confirmed that the observed resistance fluctuations are significantly non-Gaussian. This fact can be attributed to the nanostructure of the films. The estimated amplitude density depends on the gas mixture. Furthermore, the cross-level bispectra contours were characteristic signatures of the different gas mixtures. The integrated higher-order spectra can be applied as an additional source of information for gas detection, together with the power spectral density.

Acknowledgements

This research was sponsored by the U.S. Office of Naval Research. Work in the U.S.A. was supported by the Swedish Foundation for International Cooperation in Research and Higher Education (“STINT”) for J. E. and by the European Community — Access to Research Infrastructure action of the Improving Human Potential Programme for J. S.

References

- [1] L. B. Kish, R. Vajtai and C. G. Granqvist, *Extracting information from the noise spectra of chemical sensors: Electronic nose and tongue by one sensor*, *Sensors & Actuators B* **71** (2000) 55–59.
- [2] L. B. Kish, C. G. Granqvist and J. Söderlund, *Detection of chemicals based on resistance fluctuation-spectroscopy*, Swedish patent No. 9803019-0; Publ. No. 513148.
- [3] A. Hoel, J. Ederth, J. Kopniczky, P. Heszler, L. B. Kish, E. Olsson and C. G. Granqvist, *Conduction invasion noise in nanoparticle WO₃/Au thin-film devices for gas sensing applications*, *Smart Mater. Struct.* **11** (2002) 640–644.
- [4] G. Schmera and L. B. Kish, *Surface diffusion enhanced chemical sensing by surface acoustic waves*, *Sensors & Actuators B* **93** (2003) 159–163.
- [5] J. Smulko, L. B. Kish and C. G. Granqvist, *On the statistical analysis of noise in chemical sensors and its application for sensing*, *Fluctuation and Noise Letters* **1** (2001) L147–L153.
- [6] J. Smulko, L. B. Kish and G. Schmera, *Application of nonlinearity measures to chemical sensor signals*, *Proc. Soc. Photo-Opt. Instrum. Engr.* **5115** (2002) 92–100.
- [7] J. R. Mendel, *Tutorial on higher-order statistics (spectra) in signal processing and system theory: Theoretical results and some application*, *Proc. IEEE* **79** (1991) 278–305.
- [8] C. G. Granqvist and R. A. Buhrman, *Ultrafine metal particles*, *J. Appl. Phys.* **47** (1976) 2200–2219.
- [9] J. K. Tugnait, *Detection of non-Gaussian signals using integrated polyspectrum*, *IEEE Trans. Signal Proc.* **42** (1994) 3137–3149.
- [10] N. Rozario and A. Papoulis, *Transfer function phase estimation using a low variance higher-order spectrum*, *Proc. Fourth Annual ASSP Workshop on Spectrum Estimation and Modeling*, Minneapolis, August (1988) 217–221.
- [11] J. S. Bendat and A. G. Piersol, *Random Data Analysis and Measurement Procedures*, Wiley, New York (2001).